THE JOURNAL OF BIOLOGICAL CHEMISTRY VOL. 286, NO. 47, pp. 40556–40565, November 25, 2011

In Vivo Role for the Chromatin-remodeling Enzyme SWI/SNF in the Removal of Promoter Nucleosomes by Disassembly Rather Than Sliding[S]

Received for publication, August 4, 2011, and in revised form, September 6, 2011 Published, JBC Papers in Press, October 6, 2011, DOI 10.1074/jbc.M111.289918

Christopher R. Brown[1,2], **Changhui Mao**[1], **Elena Falkovskaia, Jason K. Law, and Hinrich Boeger**[3]

From the Department of Molecular, Cell, and Developmental Biology, University of California, Santa Cruz, California 95064

Background: The enzymatic activities catalyzing disassembly of promoter nucleosomes *in vivo* are unknown.
Results: We show that nucleosomes are lost from activated *PHO8* gene and promoter circles, formed *in vivo*, in an SWI/SNF-dependent manner.
Conclusion: SWI/SNF plays a role in nucleosome disassembly *in vivo*.
Significance: Our findings are the first demonstration of nucleosome disassembly *in vivo* dependent on a known chromatin-remodeling enzyme.

Analysis of *in vivo* chromatin remodeling at the *PHO5* promoter of yeast led to the conclusion that remodeling removes nucleosomes from the promoter by disassembly rather than sliding away from the promoter. The catalytic activities required for nucleosome disassembly remain unknown. Transcriptional activation of the yeast *PHO8* gene was found to depend on the chromatin-remodeling complex SWI/SNF, whereas activation of *PHO5* was not. Here, we show that *PHO8* gene circles formed *in vivo* lose nucleosomes upon *PHO8* induction, indicative of nucleosome removal by disassembly. Our quantitative analysis of expression noise and chromatin-remodeling data indicates that the dynamics of continual nucleosome removal and reformation at the activated promoters of *PHO5* and *PHO8* are closely similar. In contrast to *PHO5*, however, activator-stimulated transcription of *PHO8* appears to be limited mostly to the acceleration of promoter nucleosome disassembly with little or no acceleration of promoter transitions following nucleosome disassembly, accounting for the markedly lower expression level of *PHO8*.

Nucleosomes occlude transcription factor binding sites and inhibit the initiation of transcription *in vitro* and *in vivo* (1–5). Transcription therefore requires changes in the structure of nucleosomes that occupy essential promoter sequences. The isolation of enzymes that can break and reform histone-DNA interactions in an ATP-dependent manner provided a first answer to the question of how cells overcome nucleosomal inhibition (6).

In vitro experiments demonstrated the ability of chromatin remodelers to couple ATP hydrolysis to the sliding of nucleosomes along the DNA (7, 8), and evidence has been presented for nucleosome sliding *in vivo* (9). Although the activity of some remodelers appears to be limited to sliding, others, including SWI/SNF and its close relative RSC, were also found to catalyze the transition of mononucleosomes into a persistently altered state with increased DNA accessibility but without loss of histones (10–12), the transfer of histone octamers between DNA molecules (13, 14), and nucleosome disassembly (15, 16). Which of these activities are physiologically significant, rather than owed to the biochemical assay conditions, is unclear.

Extensive structural analysis of *in vivo* chromatin remodeling at the *PHO5* promoter of *Saccharomyces cerevisiae*, which undergoes a major transition in chromatin structure upon *PHO5* induction (17), suggested that remodeling results in loss of promoter nucleosomes. Loss was inferred from complementary quantitative results of limiting nuclease digestion analysis and topology measurements (18). Conforming with the loss hypothesis, regions occupied by nucleosomes under repressing conditions sedimented like naked DNA in a density gradient after release from the activated promoter by restriction endonuclease digestion, and chromatin immunoprecipitation experiments suggested that fewer histones were bound to the activated promoter than the repressed one (18, 19).

Chromatin circles formed *in vivo* were seen to lose nucleosomes under conditions that activate *PHO5* when encompassing the *PHO5* promoter, demonstrating the ability of the cell to catalyze nucleosome disassembly and suggesting that loss of promoter nucleosomes at the chromosomal *PHO5* locus is due to disassembly rather than sliding of nucleosomes away from the promoter (20).

The SWI/SNF complex has been implicated in histone eviction from promoter elements *in vivo* (21–23). Whether SWI/SNF-dependent eviction occurred by disassembly or sliding of nucleosomes is unknown. Deletion of *SNF2*, which encodes the catalytic subunit of the SWI/SNF complex, was found to affect expression and promoter chromatin remodeling of *PHO5* only marginally. Defects in *PHO5* expression have been reported in the absence of other remodelers, but none of them alone proved to be essential for *PHO5* activation (24–26). The catalytic activ-

[S] The on-line version of this article (available at http://www.jbc.org) contains supplemental Table 1 and Fig. 1.

[1] Both authors contributed equally to this work.

[2] Supported by National Research Service Award Grant F32GM087867 from the National Institutes of Health.

[3] Supported by National Institutes of Health Grant GM078111 and the Pew Scholars Program. To whom correspondence should be addressed: Dept. of Molecular, Cell, and Developmental Biology, University of California, 1156 High St., Santa Cruz, CA 95064. Tel.: 831-459-4487; Fax: 831-459-3139; E-mail: hboeger@ucsc.edu.

ities that promote nucleosome disassembly *in vivo* remain to be determined.

In contrast, activated expression of the *PHO8* gene of yeast, although induced by the same signaling pathway and transcriptional activator as *PHO5*, has been shown to be dependent on *SNF2* (27). The structural nature of remodeled chromatin at the *PHO8* promoter and the question of whether nucleosome loss occurs by disassembly rather than sliding are, therefore, of particular interest.

It has been argued previously that loss of nucleosomes from the *PHO8* promoter was due to disassembly rather than sliding because expression and chromatin remodeling of *PHO8* were found to require the histone chaperone Asf1 (28), which earlier had been implicated in replication-dependent nucleosome assembly (29). This argument implicitly assumed that Asf1 facilitates nucleosome disassembly. However, independent evidence to support this assumption has not been presented, and subsequent biochemical tests failed to provide such evidence (16).

Here, we addressed the question of whether nucleosomes are removed from the induced *PHO8* promoter by disassembly rather than sliding. Our findings are consistent with removal of nucleosomes by disassembly, but not sliding. We observed that Snf2 was essential for disassembly of promoter nucleosomes at *PHO8*. Together with recent biochemical analyses, our findings support the notion that SWI/SNF catalyzes nucleosome disassembly *in vivo*.

EXPERIMENTAL PROCEDURES

Plasmids and Strains—For a complete list of strains used in this study, see supplemental Table 1. The *PHO8* gene, including 1500 bp upstream of the start codon and 710 bp downstream of the stop codon, was cloned by PCR and inserted into the NotI site of pM47.1 (18), generating plasmid pM75.2. Introduction of an NruI site in place of the EcoRI site most proximal to the 5′-end of the *PHO8* open reading frame (ORF) yielded plasmid pM77.2. Deletion of a 2.93-kb NruI fragment from plasmid pM77.2, encompassing the *PHO8* promoter and ORF, and its replacement with a 1.1-kb fragment bearing the *URA3* gene generated plasmid pM78.5. The *PHO8* gene circle plasmid pM79.44 was constructed in a way similar to that for the *PHO5* gene circle plasmid (18). One recombination sequence (RS)[4] element was inserted into the NruI site upstream of the ORF, and the other RS element and LexA cluster were inserted into the downstream NruI site on pM77.2. In pM79.44 the sequence 5′-TAGTATATAAAGAAAGAAGTGTA-3′ was replaced with 5′-TCATCGATCCCCCGGGGGACGAGT-3′, which replaced the *PHO8* TATA box and downstream promoter sequences with cleavage sites for restriction endonucleases ClaI and SmaI yielding the *PHO8* gene circle plasmid pM82.1. The *PHO8* promoter circle plasmid pCM110.1 was derived from pM75.2 and pM82.1 by inserting the downstream RS element and LexA cluster into the SacI site 56 bp downstream of the start codon. Pho4 activation domain mutants were constructed as described previously (30).

The *PHO8* gene was replaced with *URA3* by homologous recombination in strains YS18 and yM7.8 using plasmid pM78.5, generating strains yM51.1 and yM52.2, respectively. *PHO8* gene circle strains yM53.78 and yM54.9 were generated by replacing *pho8::URA3* in strains yM51.1 and yM52.2 with the TATA-less *pho8* gene circle construct on plasmid pM82.1. The *pho4* deletion strain yM59.20 was generated by replacing *PHO4* with *URA3*. Strain yM120.2 was generated from strain yM54.9 by replacing *PHO4* with *URA3* from plasmid pCM4.5. The *PHO4* activation domain mutation strains were derived from strain yM120.2 as described previously (30). The *PHO8* promoter circle strain yC104.34 was derived from strain yM52.2 by replacing *pho8::URA3* with a *pho8* promoter circle from plasmid pCM110.1. Strain yC192.1 was generated from yC104.34 by replacing *PHO4* with *URA3* using plasmid pCM4.5. Strain yE22.1 was generated by replacing the *PHO5*p:*CFP* cassette in strain yE2.1 with *URA3*. Exchanging *LEU2* in the *PHO80* locus of yE22.1 with *HIS3* generated strain yC57.10. The *PHO5* gene circle strain yC59.11 was then generated by replacing *URA3* in yC57.10 with the *PHO5* gene circle construct using plasmid pM70.1 (18), and replacement of *PHO4* with *URA3* in yC59.11 gave strain yC87.2.

PHO8 promoter and *CFP* ORF sequences were fused at the *PHO8* start codon by overlapping PCR (31), using plasmids pM75.2 (see above) and 14846 (Addgene) as templates. The *PHO8p:CFP* fusion was used to replace a 2.3-kb EcoRV-SalI fragment in pM75.2 bearing the *PHO8* gene, including its promoter, except for the last 3′-terminal 238 bp of the ORF, generating plasmid pJL2.2. Plasmid pJL3.4, which bears the fusion between the *PHO8* promoter and *YFP* ORF, was constructed analogously. *YFP* ORF sequences were amplified by PCR from plasmid 14840 (Addgene). The wild-type *PHO5* gene was restored in strains yC56.11 and yC57.10 (30) using plasmid pM50.1 (18) to generate strains yJL5.7 and yJL4.4, respectively. The *PHO8* gene in these two strains was then replaced with *URA3* using plasmid pM78.5 to generate strains yJL7.4 and yJL6.4. Strains yJL8.1 and yJL9.1 were then derived from yJL6.4 and yJL7.4 by homologous recombination with plasmids pJL2.2 and pJL3.4, respectively, replacing *pho8::URA3* with *PHO8p:CFP* and *PHO8p:YFP*. Strain yJL12.1 was generated from strain yJL9.1 by knocking out *PHO4* with *URA3* using plasmid pCM4.5. The diploid strain yJL10.1 was generated by mating yJL8.1 and yJL9.1.

An *asf1::KanMX* knock-out cassette was amplified from a heterozygous diploid (GSA-6 Heterodiploid Knock-out Collection, ATCC) using primers 5′-AATGCTGTTTTATTCCGTTCTTACA-3′ and 5′-GATTTTTATTCCAACATGTTCGTTC-3′. The appropriate band was purified and used to transform *PHO8* and *PHO5* gene circle strains yM53.78, yM54.9, and yC58.8, yC59.11, yC72.1, and yC87.2, respectively, creating strains CBY11.4, CBY12.1, and yC117.1, yC118.1, yC119.1, and yC120.1, respectively. A *snf2::KanMX* knock-out cassette was amplified from a heterozygous diploid (GSA-6 Heterodiploid Knock-out Collection, ATCC) using primers 5′-TTAATTCCAATACATTCGCCACTAT-3′ and 5′-CAAGAACAAGTTCACTATGATGACG-3′. The appropriate

[4] The abbreviations used are: RS, recombination sequence; CFP, cyan fluorescent protein; MNase, micrococcal nuclease; RSC, remodel the structure of chromatin.

band was purified and used to transform *PHO8* gene circle strains yM53.78, yM54.9, and yM59.20, creating strains CBY14.5, CBY15.5, and CBY16.1, respectively. The *snf2::KanMX* knock-out cassette was also used to transform *PHO5* gene circle strains yM63.19 and yM19.2 (30), creating strains yC45.3 and yC44-1, respectively. A *SNF2* expression plasmid, pSR127 (kindly supplied by Fred Winston, Harvard University), was used to transform strains CBY14.5, CBY15.5, and CBY16.1, creating strains CBY14.5P, CBY15.5P, and CBY16.1P, respectively. All yeast transformations were performed using the lithium acetate method.

Limiting Digestion Analysis—Strains yM53.78 and yM54.9 were grown overnight in 500 ml of 2×SCR-L medium to a density of 3×10^7 cells/ml. Upon reaching this density, 50 ml of each culture was removed and placed into a new flask, to which 5 ml of 20% galactose was added to induce *PHO8* gene circle formation. These smaller cultures were allowed to incubate for an extra 1.5 h in the presence of 2% galactose, after which topoisomers were isolated as described previously (18). Nuclei were prepared from the remaining 450-ml cultures as described previously (18, 32). Frozen nuclei pellets were resuspended in micrococcal nuclease (MNase; Sigma) buffer (15 mM Tris, pH 8, 50 mM NaCl, 1 mM $CaCl_2$, 5 mM β-mercaptoethanol) and divided into 5 equal volumes to be digested with 0, 0.5, 1, 2, or 4 units of MNase for 20 min at 37 °C. Undigested (0 unit) samples were subsequently digested with either ApaLI and HaeIII (yM53.78) or EcoRV and XhoI (yM53.78 and yM54.9) to cut out a 941-bp or 930-bp fragment of the *PHO5* or *PHO8* promoter, respectively. MNase-digested samples and cut promoter fragments were run on a 1% agarose gel and prepared for Southern blotting. Blots were first probed with a 690-bp *PHO8* probe spanning the four putative promoter nucleosome positions (27). Primers used to generate the *PHO8* promoter probe were P164 5′-TCAAGAATGGCACTATAAGTGTGG-3′ and P165 5′-GCTAATGCGCGTTCAAATAATGTC-3′. Blots were stripped and rehybridized with a 690-bp *PHO5* probe spanning *PHO5* promoter nucleosomes N-1 to N-4 (33). Primers used to generate the *PHO5* promoter probe were P232 5′-GGTCCGCTCCTTCTAATAATCG-3′ and P15 5′-TGGTAATCTCGAATTTGCTTG-3′. The signal from the EcoRV/XhoI-digested *PHO8* promoter (yM53.78) probed with P164/P165 was compared with the ApaLI/HaeIII-digested *PHO5* promoter (yM53.78) probed with P232/P15 to normalize the signal intensity of the two different probes. MNase profiles for yM53.78 were used to generate a limiting value to compare the absolute number of nucleosomes on the *PHO8*- and *PHO5*-repressed promoters (*PHO8* probe signal/*PHO5* probe signal). To determine the number of nucleosomes remaining on the activated *PHO8* promoter we first normalized the *PHO8* promoter signal from yM53.78 and yM54.9 (using the EcoRV/XhoI-digested promoter samples from strains yM53.78 and yM54.9) prior to taking the yM53.78/yM54.9 signal ratio.

Topoisomer Analysis—Analysis of topoisomer distributions was performed as described previously (18, 34). *PHO8* and *PHO5* gene and promoter circle strains all bore a mutated TATA box.

Phosphatase Assay—Phosphatase assays were performed as described previously (5).

Northern Blot Analysis—Northern blot analysis was performed as described previously (30).

Expression Analysis by FACS—*PHO5* and *PHO8* promoter-controlled YFP expression was measured in live haploid cells by flow cytometry (BD Influx, BD Biosciences). The YFP proteins were excited by an air-cooled Solid State "Sapphire" (Coherent), 200-mW, 488-nm laser. The level of expression for each strain was referenced to strain $PHO5^A$ (yE1.1) (*PHO4 pho80*Δ), which was always analyzed in parallel. The level of yE1.1 expression was set to 100%. Strain yE3.1 (*pho4*Δ *pho80*Δ) was employed as a negative control to measure the level of autofluorescence and set to 0% level of expression. The YFP fluorescence was collected in the 531/40-nm channel.

For the expression analysis, cells were grown in SCD medium. Data from 100,000 cells were collected for each measurement; each sample was remeasured at least four times. No fewer than two independent cell cultures at two different cell density levels were evaluated for each strain.

Data from flow cytometry measurements were exported into FSC3.0 files, and data analysis was carried out by FlowJo software (Tree Star). To ensure sufficient data quality, data were analyzed in FSC and SSC channels, and scatters were rejected. Outliers were identified visually in the YFP channel. These procedures reduced the number of cells by 20–25%. Further reduction in cell number by imposing more stringent selection criteria did not significantly change relative expression levels.

Fluorescence Microscopy and Expression Noise Measurements—CFP and YFP expression under control of the *PHO8* promoter were measured in single diploid cells by quantitative fluorescence microscopy (30). CFP and YFP fluorescence signals for individual cells were divided by the mean CFP and YFP signal, respectively, and plotted in a scatter plot. The intrinsic noise is given by the mean squared distance of points from the diagonal of the plot (coefficient of variation squared). The intrinsic noise was determined from four independent measurements of at least 250 cells each. The variability in intrinsic noise between samples was larger than observed previously for *PHO5* (30), consistent with larger variations in expression and topology measurements, too (see below).

Computation and Modeling—Predictions of *PHO8* expression noise were made using the previously described stochastic model of *PHO5* gene expression (30). Adjustments are outlined under "Results." Calculations were performed using Mathematica 7 (Wolfram Research).

RESULTS

Transcription of *PHO8* and *PHO5* is activated upon sequence-specific binding of the transcriptional activator Pho4 at specific promoter elements (35). Entry of Pho4 into the nucleus is inhibited by the cyclin-cyclin-dependent kinase complex Pho80/Pho85. Lack of inorganic phosphate in the medium results in inhibition of the Pho80/Pho85 kinase and translocation of Pho4 into the nucleus. Thus, cells that lack Pho80 activate *PHO8* constitutively, whereas cells that lack Pho4 fail to activate *PHO8* under inducing conditions. To approach steady-state conditions as closely as possible, induced *PHO8* promoter chromatin was analyzed, unless indicated oth-

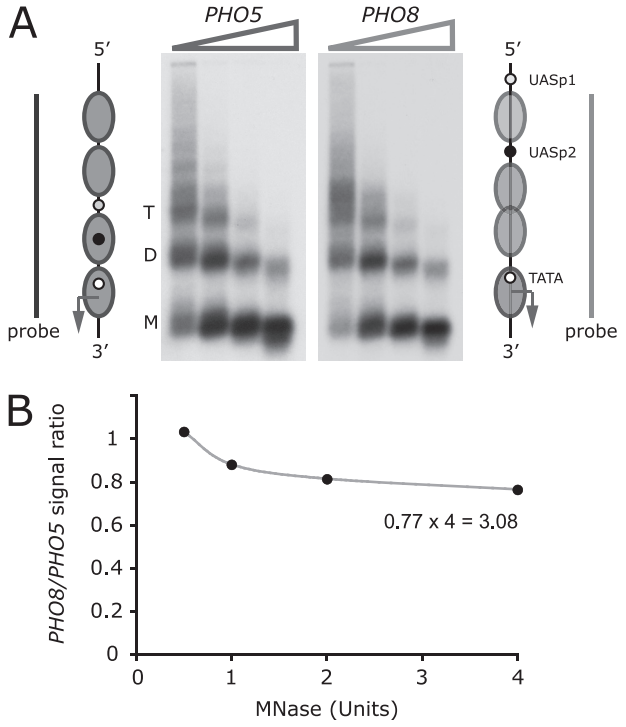

FIGURE 1. **The repressed *PHO8* promoter is occupied by three nucleosomes.** *A*, schemes of the repressed *PHO5* and *PHO8* chromatin structures (32, 36). Chromatin of noninduced cells was digested with increasing concentrations of MNase. The isolated DNA was fractionated by agarose gel electrophoresis, blotted, and sequentially hybridized with ^{32}P-labeled DNA probes spanning the *PHO5* or the *PHO8* promoter (*bars*). Positions of bands corresponding to nucleosome trimers (*T*), dimers (*D*), and monomers (*M*) are indicated. *B*, radioactivity signals integrated over the entire *lane* for each enzyme concentration. The ratio of *PHO8* and *PHO5* promoter probe signals corrected for differences in probe activity was plotted as a function of enzyme concentration.

erwise, in *pho80*Δ cells cultured in phosphate-containing media.

The Noninduced PHO8 Promoter Is Occupied by Three Nucleosomes Rather Than Four—The noninduced *PHO8* promoter is believed to be occupied by four nucleosomes, three of which were proposed to be partially unfolded to account for elevated restriction enzyme accessibilities (36). To test this hypothesis, we analyzed *PHO8* and *PHO5* promoter chromatin by limiting digestion analysis (18). To this end, we partially digested nuclei from noninduced cells with increasing concentrations of MNase, which preferentially digests linker DNA. The amount of undigested promoter DNA was measured by hybridization with ^{32}P-labeled *PHO5* and *PHO8* promoter DNA probes after gel electrophoresis and Southern blotting of isolated DNA (Fig. 1*A*). Both probes spanned a four-nucleosome-wide domain (Fig. 1*A*). The same domains were released from genomic DNA by restriction endonuclease digestion and run on the same gel as the MNase-digested DNA (data not shown). This allowed us to account for differences in probe activity.

The ratio of undigested *PHO8* and *PHO5* promoter DNA reached a limiting value of 0.77 ± 0.1 (two independent experiments) at high enzyme concentrations (Fig. 1*B*). The low restriction enzyme accessibilities of sequences occupied by nucleosomes suggest that nucleosome positions are close to fully occupied at the repressed *PHO5* promoter (17). Thus, the limiting value indicated that the noninduced *PHO8* promoter is occupied, on average, by $0.77 \times 4 = 3.1$ nucleosomes that are equally resistant to MNase attack as nucleosomes at the *PHO5* promoter. Notably, the length of DNA protected against MNase attack was identical for the nucleosomes of both promoters (Fig. 1*A*). The paucity of distinct digestion products shorter than the expected length of the nucleosome core particle argued against the existence of stable, partially unfolded nucleosomes. Differences in the cleavage frequencies of restriction endonucleases are likely to reflect differences in nucleosome occupancy rather than structure. The same conclusion was reached for activated *PHO5* promoter chromatin (18).

Chromatin Remodeling Removes Nucleosomes from the Induced PHO8 Promoter—Loss of nucleosomes from the induced *PHO8* promoter was previously inferred from nuclease accessibility and chromatin immunoprecipitation assays (28, 36). However, the existence of stable partially unfolded nucleosomes may be, and has been (see above), invoked to explain elevated nuclease accessibility, and nucleosome-bound remodelers that encapsulate the nucleosome upon binding, such as RSC (37–39), may interfere with cross-linking of histones to DNA or the recognition of histone epitopes by antibodies.

To clarify the structural nature of induced *PHO8* promoter chromatin, we compared activated and repressed promoter chromatin at steady state by limiting digestion and topology analyses. For these experiments, we used strains in which the *PHO8* gene or promoter was flanked by the recognition sequences for the site-specific R recombinase of *Zygosaccharomyces rouxii*, which was expressed under control of the inducible *GAL1* promoter (40). The position of the upstream RS is indicated in Fig. 2*A*. The second RS element was inserted 250 bp downstream of the *PHO8* stop codon for gene circles or 56 bp downstream of the *PHO8* start codon for promoter circles. Recombination results in removal of the *PHO8* gene in circular form from its chromosomal locus. To exclude topological effects due to transcription (18), strains furthermore bore a mutation in the *PHO8* TATA box.

The digestion of equal amounts of activated and repressed promoter chromatin with increasing concentrations of MNase showed that the ratio between activated and repressed promoter DNA reached a limiting value of 0.41 ± 0.1 (Fig. 2*A*, two independent experiments). Assuming that the repressed promoter bears three nucleosomes, on average, this result suggests that about $0.4 \times 3 = 1.2$ nucleosomes are retained at the activated promoter, equally resistant to MNase attack and protecting the same length of DNA as repressed promoter nucleosomes (Fig. 2*A*).

What was the fate of the 1.8 altered nucleosomes? To address this question, we induced formation of *PHO8* gene circles in the same cultures that were used for limiting digestion analysis and isolated gene circle DNA topoisomers. If the altered nucleosomes unfolded completely, the linking difference between activated and repressed circles should be similar to the number of altered nucleosomes, given that nucleosome formation on a closed DNA circle reduces the linking number of the DNA circle by about −1/nucleosome in relaxation equilibrium (41–43). Topoisomer distributions were resolved by chloroquine-aga-

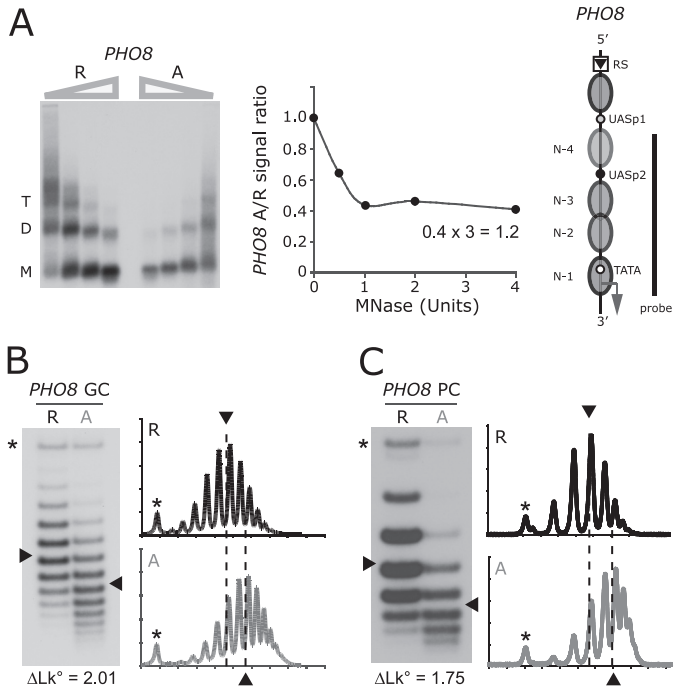

FIGURE 2. **Nucleosomes are removed from the induced *PHO8* promoter.** *A*, repressed (*R*) and activated (*A*) *PHO8* promoter chromatin digested with increasing concentrations of MNase. The isolated DNA was fractionated by agarose gel electrophoresis, blotted, and hybridized with a ^{32}P-labeled DNA probe spanning the *PHO8* promoter. The signal:ratio for DNA from activated and repressed cells on corresponding *lanes* was plotted as a function of enzyme concentration. The position of the upstream recombination sequence, *RS*, is indicated on the *PHO8* promoter diagram to the *right*. *B*, topoisomer analysis of repressed and activated *PHO8* gene circles (*GC*). DNA topoisomers were resolved by gel electrophoresis in the presence of chloroquine (18), blotted, and hybridized with a ^{32}P-labeled DNA probe spanning the *PHO8* gene. The linking number of topoisomers increases from *top* to *bottom*. An *asterisk* indicates the position of nicked circles. *Line profiles* of the topoisomer distributions are shown to the *right* of each blot. Δ*Lk* refers to the linking difference measured between the centers of the topoisomer distributions of activated and repressed *PHO8* gene circles. *C*, topoisomer analysis of repressed and activated *PHO8* promoter circles (*PC*) spanning five nucleosome positions.

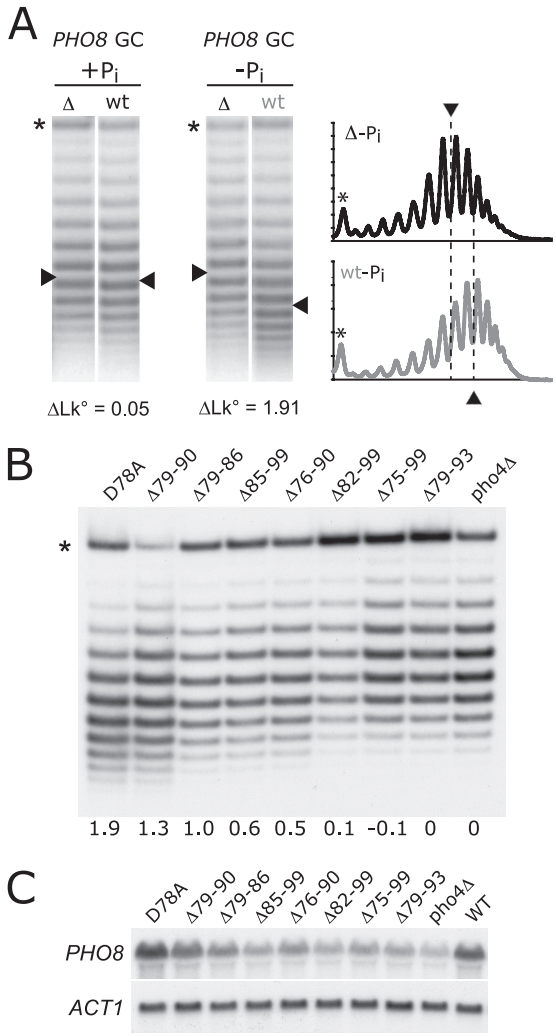

FIGURE 3. **Nucleosomes continually disassemble and reassemble at the activated *PHO8* promoter.** *A*, *PHO8* gene circles (*GC*) formed in *pho4*Δ (Δ) or *PHO4* (*wt*) cells cultured in high phosphate media. Topoisomers were obtained from cells either before (+*Pi*) or after (−*Pi*) transfer of cells into phosphate-free medium, separated by gel electrophoresis, blotted, and hybridized as described above (Fig. 2). The linking difference of 0.05 for repressed circles is within the margin of measurement error and sample variability, but may also be explained by the finding that Pho4 briefly enters the nucleus during S phase under repressing conditions (50). Δ*Lk* refers to the linking difference measured between the centers of the topoisomer distributions of activated and repressed *PHO8* gene circles. *B*, topoisomer distributions of *PHO8* gene circles formed in strains bearing mutations in the activation domain of the Pho4 activator. Mutants are arranged, from *left* to *right*, in order of decreasing activator strength (*PHO8* expression level, see *C*). Linking differences relative to repressed *PHO8* (*pho4*Δ) gene circles are indicated at the *bottom* of the image. *C*, Northern blot analysis of *PHO8* expression in *pho4* mutants. *ACT1* mRNA was used as a loading control.

rose gel electrophoresis, blotted, and hybridized with a ^{32}P-labeled DNA probe encompassing the *PHO8* gene. The average linking difference between the topoisomers of the activated and repressed gene circles was indeed closely similar to the number of altered nucleosomes determined by limiting digestion analysis (Fig. 2*B*). For unknown reasons, linking differences between *PHO8* gene circles varied more strongly than observed previously for *PHO5* gene circles (18). However, the average linking difference of 1.82 (S.D. ± 0.33) from 20 measurements of 10 independent preparations was in excellent agreement with our expectation for complete unwrapping of DNA from the altered nucleosomes.

Topology analysis of promoter circles that encompass promoter nucleosome positions N-1 to N-4 (Fig. 2*A*) plus sequences for one additional upstream nucleosome led to a similar result (Fig. 2*C*). We found an average linking difference between activated and repressed circles of 1.61 (S.D. ± 0.28), suggesting that most if not the entire linking difference between activated and repressed gene circles was due to changes in promoter chromatin.

Removal of PHO8 Promoter Nucleosomes Occurs by Disassembly Rather Than Sliding—Promoter nucleosomes may be removed either by sliding away from the promoter or by disassembly. To distinguish between both possibilities, we formed *PHO8* gene circles in *pho4*Δ and *PHO4* wild-type cells grown in high phosphate medium and isolated topoisomers before and after transfer of cells into phosphate-free medium. As expected, topoisomer distributions from both cell types were virtually identical prior to transfer of cells into phosphate-free medium (Fig. 3*A*). However, after incubation of cells in phosphate-free medium, the average linking number of *PHO8* circles in *PHO4*

wild-type cells increased relative to circles from *pho4*Δ cells by 1.9 (Fig. 3*A*), suggesting the loss of about 2 nucleosomes from induced *PHO8* circles. Removal of promoter nucleosomes by sliding away from the promoter would have preserved the number of circle nucleosomes and the circle linking number.

Nucleosome Disassembly Is Counterbalanced by Reassembly—On average, the activated *PHO8* promoter is not nucleosome-free (Fig. 2*A*). What is the mechanism that retains promoter nucleosomes? The simplest possibility, perhaps, is that disassembly is counterbalanced by reformation of nucleosomes (18). If nucleosomes reformed under activating conditions, mutations in the Pho4 activation domain, which is essential for promoter chromatin remodeling (44), were expected to shift the equilibrium gradually between nucleosome removal and reformation. If reassembly did not occur, the maximal number of nucleosomes would always be removed, even in cells expressing weak activators, albeit at a slower rate. We determined the extent of nucleosome loss from the induced *PHO8* promoter by topology analysis in eight *pho80*Δ strains that bore different mutations in the Pho4 activation domain (30). Linking differences between activated and repressed gene circles gradually decreased with decreasing activator strength (Figs. 3, *B* and C; see also Fig. 7*D*), as predicted by the reformation hypothesis. This result conformed to previous topology measurements of *PHO5* promoter chromatin remodeling (30) and was consistent with the observation of genome-wide histone exchange at promoters (45).

Disassembly of PHO8 Promoter Nucleosomes Requires Swi2 but Not Asf1—Changes in nuclease accessibility of *PHO8* promoter chromatin have previously been shown to require Snf2 (27). Thus, linking changes in gene circles due to *PHO8* induction should also depend on Snf2. To test this prediction, we repeated our topology analysis of activated and repressed *PHO8* gene circles in *snf2*Δ cells. As predicted, deletion of *SNF2* markedly interfered with nucleosome removal in *pho80*Δ cells (Fig. 4*A*). The linking difference between activated and repressed *PHO8* gene circles decreased by 95% to 0.087 (with a S.D. ± 0.25 in four independent experiments). In contrast, deletion of *ASF1* had little effect on nucleosome disassembly in *pho80*Δ cells (linking difference 1.68 ± 0.11 in two independent experiments, Fig. 4*B*), suggesting that the rate of nucleosome disassembly at steady state was either hardly affected or that the rates of disassembly and reassembly were equally altered.

Similarly, deletion of *ASF1* in *PHO5* gene circle strains had little effect on the linking difference between activated and repressed circles isolated from *pho80*Δ and *PHO80* cells, respectively (linking difference 1.81 ± 0.25 in four independent measurements and two different strains; see supplemental Fig. 1).

Disassembly of PHO5 Promoter Nucleosomes Can Be Dependent upon SNF2—In pursuit of the possible cause for the different coactivator dependences of *PHO5* and *PHO8*, we unexpectedly found, in the same strains as those used for *PHO8* gene circle formation, that constitutive *PHO5* expression in *pho80*Δ cells was abolished upon deletion of *SNF2* (Fig. 5*A*). The activation defect could be fully suppressed by transforming *snf2*Δ cells with a *SNF2* expression plasmid, ruling out the possibility that other genes critical for *PHO5* expression had accidentally been damaged upon *SNF2* deletion (Fig. 5*A*). A similar result was obtained in *PHO80* wild-type cells, induced by transfer into phosphate-free medium (Fig. 5*A*). Only after long periods of phosphate starvation, and even then in only half of our experiments (two of four replicates), did we observe a transient Pho4-dependent increase in *PHO5* expression in *snf2*Δ cells (Fig. 5*A*). In contrast, *PHO5* expression in *SNF2* wild-type cells decreased when cultured for long times in phosphate-free medium, raising the possibility that Snf2, depending on the physiological context, may function as a repressor as well as a coactivator of *PHO5* expression.

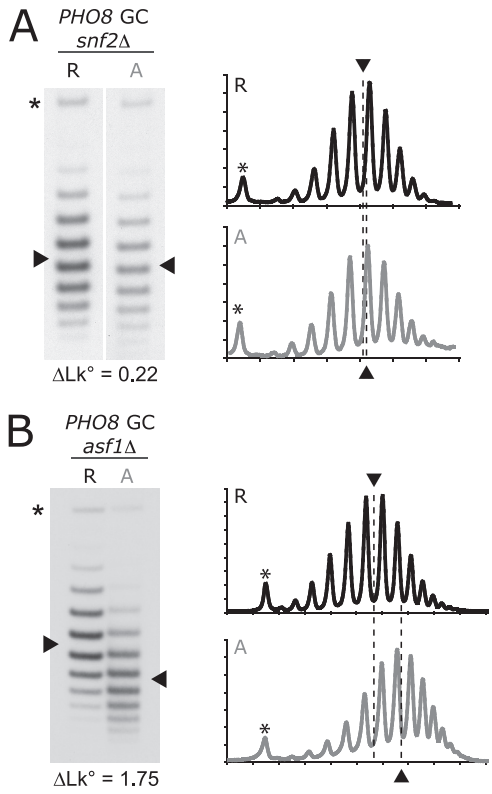

FIGURE 4. **Nucleosome removal from the *PHO8* promoter requires Snf2 but not Asf1.** *A*, topoisomer analysis of repressed (*R*) and activated (*A*) *PHO8* gene circles (*GC*) in *snf2*Δ cells. *B*, topoisomer analysis of repressed and activated *PHO8* gene circles isolated from *asf1*Δ cells. Δ*Lk* refers to the linking difference measured between the centers of the topoisomer distributions of activated and repressed *PHO8* gene circles.

The linking difference between activated and repressed *PHO5* gene circles, isolated from *pho80*Δ and *pho80*Δ *pho4*Δ cells, respectively, was 1.85 in the presence of Snf2, conforming with earlier measurements, but only 0.18 in its absence (Fig. 5, *B* and *C*), consistent with the observed expression defect of *PHO5* in *snf2*Δ cells (Fig. 5*A*).

By deleting *SNF2* in other strain backgrounds, we confirmed earlier results of others that *PHO5* can be activated in the absence of *SNF2* (46), suggesting that the effect observed here was strain-specific (data not shown).

Activated PHO8 Expression Is Caused Primarily by Accelerated Promoter Nucleosome Disassembly—To compare promoter strengths, we measured expression of yellow fluorescent protein (YFP) from either the *PHO5* or the *PHO8* promoter using flow cytometry. Under repressing conditions, *PHO8p:YFP* expression exceeded *PHO5p:YFP* expression 4-fold, con-

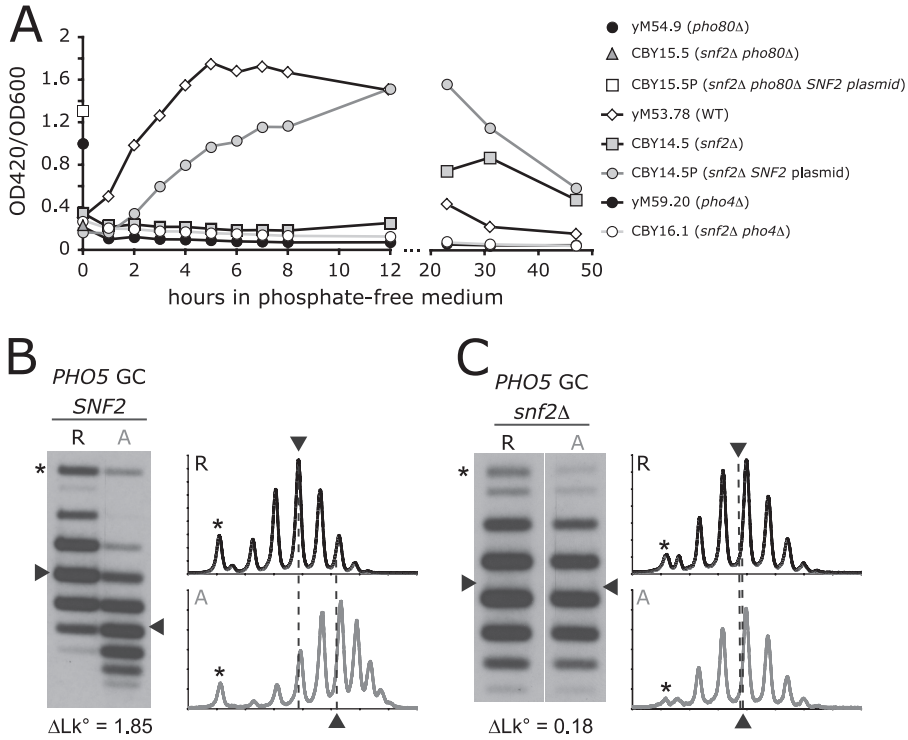

FIGURE 5. ***SNF2* is required for *PHO5* expression and promoter nucleosome removal.** *A*, *PHO5* encodes a secreted acidic phosphatase and accounts for 90% or more of the cellular acidic phosphatase activity upon induction (59). Phosphatase activity was measured in *pho80*Δ cells grown in high phosphate medium and in *PHO80* wild-type cells after incubation for different times in phosphate-free medium. *B*, topoisomer distributions of repressed (*R*) and activated (*A*) *PHO5* gene circles (*GC*) isolated from *pho80*Δ *pho4*Δ *SNF2* and *pho80*Δ *SNF2* cells, respectively. *C*, topoisomer distributions of repressed and activated *PHO5* gene circles isolated from *pho80*Δ *pho4*Δ *snf2*Δ and *pho80*Δ *snf2*Δ cells, respectively. Δ*Lk* refers to the linking difference measured between the centers of the topoisomer distributions of activated and repressed *PHO5* gene circles.

sistent with the assumption of partial derepression due to the lower nucleosome occupancy of the noninduced *PHO8* promoter (see above). In contrast, expression of *PHO8p:YFP* in *pho80*Δ cells amounted to only 7.5% of *PHO5* promoter-controlled expression (Fig. 6), although both promoters lose about two nucleosomes upon induction. How can the difference between expression levels be explained?

Because nucleosomes interfere with transcription factor binding at promoter elements and transcriptional initiation, fluctuations in promoter nucleosome occupancy contribute to the fluctuation in gene expression (expression noise). The quantitative relationship among *PHO5* promoter nucleosome loss, expression level, and noise was explained on the basis of a stochastic model of chromatin remodeling and gene expression, assuming that promoter nucleosome disassembly and preinitiation complex formation ("promoter activation") are the rate-limiting, activator-controlled, steps of *PHO5* expression (30).

The *PHO5* and the *PHO8* promoters lose the same numbers of nucleosomes upon induction, consistent with similar rates of nucleosome disassembly. Given the markedly lower level of *PHO8* expression, this suggested that promoter activation is much less efficient at *PHO8* than *PHO5*. We therefore speculated that activated *PHO8* expression is due only to the acceleration of promoter nucleosome disassembly but not promoter activation, in contrast to *PHO5* (30).

To test this hypothesis, we employed the *PHO5* model, with kinetic parameter values previously derived from *PHO5* noise and chromatin structure analyses (30), to predict the noise of

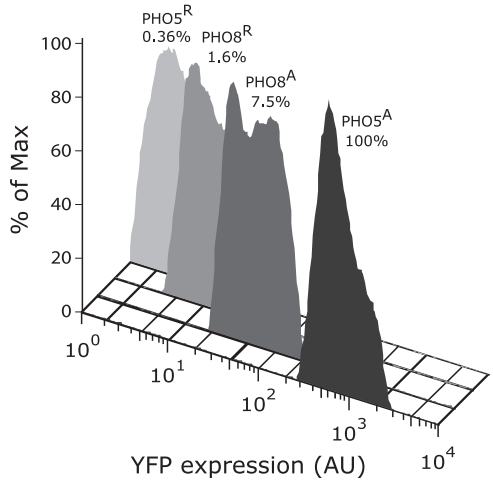

FIGURE 6. **Flow cytometry analysis of relative YFP expression under control of the *PHO8* or *PHO5* promoter in *pho80*Δ *pho4*Δ (*R*) or *pho80*Δ (*A*) cells.** Mean values of expression distributions are indicated relative to *PHO5* promoter-controlled expression in *pho80*Δ cells ($PHO5^A$, 100%). *AU*, arbitrary units.

PHO8 expression, and then we compared predicted and measured noise. We took into account that replacement of the *PHO8* core promoter with the *PHO5* core promoter increased *PHO8* expression 1.7-fold (47), suggesting that general transcription factors bind more tightly to the *PHO5* promoter. In the *PHO5* model, we therefore increased the rate of transitions out of the transcriptionally active state accordingly (Fig. 7*A*, parameter *i*) before calculating noise values for *PHO8* expression. The tuning of the kinetic parameter for promoter activation in the

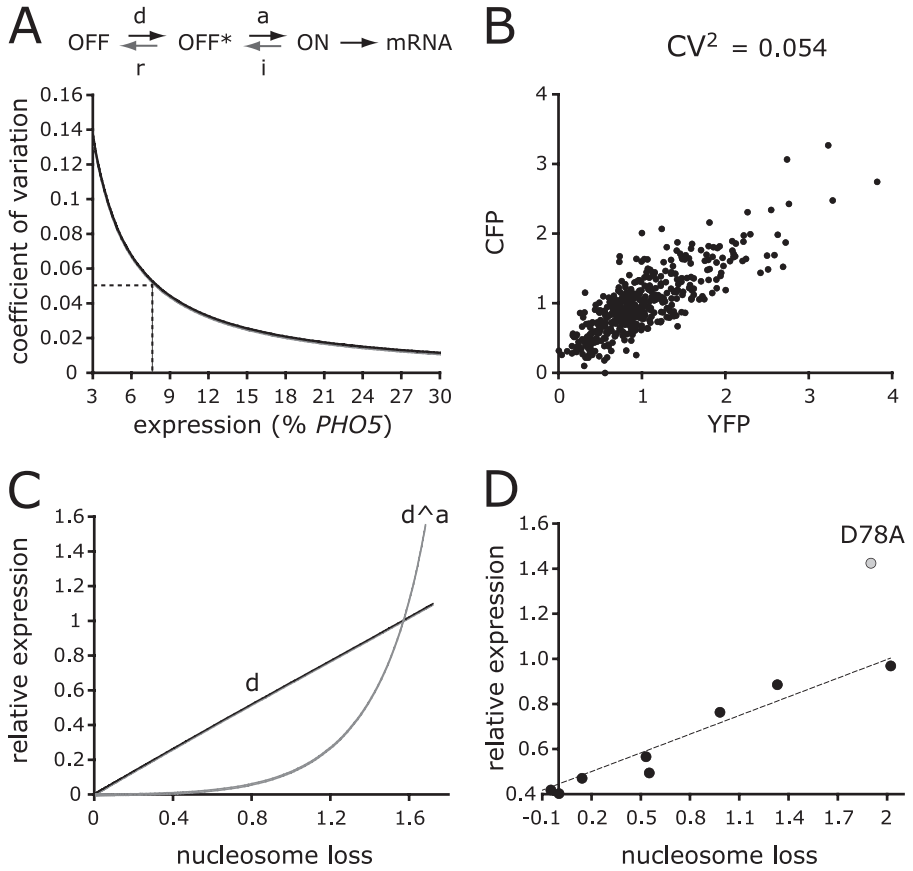

FIGURE 7. **Predicting the profile of *PHO8* promoter nucleosome loss and the intrinsic noise of *PHO8* expression.** *A*, expression noise (variance divided by the squared mean, coefficient of variation) and the mean of expression calculated using a stochastic model of *PHO5* promoter chromatin remodeling and expression with kinetic parameter values derived from *PHO5* noise and chromatin structure data (30). The model assumes three functional promoter states (see scheme): OFF (core promoter occupied by a nucleosome, transcriptionally inactive), OFF* (no nucleosome at the core promoter, transcriptionally inactive), and ON (no nucleosome at the core promoter, transcriptionally active). For details, see Ref. 30. For predicting *PHO8* expression noise, we modified the *PHO5* model to account for the observation that exchange of the *PHO8* core promoter for the *PHO5* core promoter increased *PHO8* expression 1.7-fold (47). The reverse exchange should therefore decrease *PHO5* expression by a factor of 1.7. We interpreted the difference in core promoter strength in terms of the stability of general transcription factor complexes and thus decreased the kinetic parameter for transition out of the ON state (*i*) to reduce the level of expression by a factor of 1.7. Noise and expression were then calculated for values of the kinetic parameter for promoter activation (*a*) between zero and the *PHO5* wild-type value of *a* (30). The calculation predicted a noise value of 0.053 at 7.5% of *PHO5* wild-type expression, the relative expression level of *PHO8* (Fig. 6). *B*, the intrinsic noise of *PHO8* expression determined by measuring abundances of YFP and CFP in single diploid cells, expressing both chromophores under control of the *PHO8* promoters. *Single dots* indicate YFP and CFP abundances in individual cells. Abundances were determined by quantitative fluorescence microscopy and normalized to the mean abundance of each chromophore within the analyzed cell population. The average measured noise value was 0.054. *C*, the adjusted *PHO5* model (*A*) was used to calculate the quantitative relationship between promoter nucleosome loss and expression (relative to wild type) by either tuning the kinetic parameter for nucleosome disassembly alone (curve *d*) or equally tuning the parameters for nucleosome disassembly and promoter activation (curve $d \wedge a$). *D*, plot of expression (mRNA) and nucleosome loss data (linking differences) shown in Fig. 3.

PHO5 model (Fig. 7*A*, parameter *a*) generated a noise profile predicting a noise value of 0.053 at the *PHO8* expression level, 7.5% of *PHO5* expression (Fig. 7*A*, *6*).

To measure the intrinsic noise of *PHO8* expression (48), we constructed a diploid *pho80*Δ strain that expresses YFP and CFP under control of the *PHO8* promoter. CFP and YFP expression in single cells was analyzed by quantitative fluorescence microscopy. Plotting YFP against CFP expression generates a scatter plot for a population of cells (Fig. 7*B*). With fluorescent signals normalized to a mean of 1, the intrinsic noise equals the mean squared distance of points from the plot diagonal (49). We found a noise value of 0.054 (±0.018) for *PHO8* expression (Fig. 7*B*), in excellent agreement with the theoretical prediction of 0.053 (Fig. 7*A*).

If indeed Pho4 controlled the rate of nucleosome disassembly, but not promoter activation, a linear relationship between promoter nucleosome loss and expression was expected (Fig. 7*C*, curve *d*). In contrast, if Pho4 controlled the rates of nucleosome disassembly and promoter activation, a nonlinear function was predicted (Fig. 7*C*, curve $d \wedge a$). Consistent with the first assumption and our noise analysis, the data shown in Fig. 3, *B* and *C*, were best approximated by a linear graph (Fig. 7*D*). Only the data point for the gain-of-function mutation D78A was poorly explained by this linear approximation.

DISCUSSION

By limiting digestion, topology, and expression noise analyses, we provided evidence corroborating the following conclusions. The noninduced *PHO8* promoter is occupied by three normally folded nucleosomes rather than four nucleosomes of which some are partially unfolded. Chromatin remodeling upon *PHO8* induction removes nucleosomes from the activated promoter. Removal occurs by disassembly in a Snf2-dependent manner and is counterbalanced by continuous refor-

mation of nucleosomes. Disassembly does not require the histone chaperone Asf1. Activated expression of *PHO8*, in contrast to *PHO5*, is due primarily to accelerated promoter nucleosome disassembly.

The observed defect in nucleosome removal from the activated *PHO5* promoter in *snf2*Δ cells was surprising, given previous reports that *PHO5* expression can be induced in the absence of Snf2 (46). However, SWI/SNF has been implicated earlier in *PHO5* expression. *PHO5* was found to be weakly expressed during S phase, in high phosphate media (50). This expression required Pho4 as well as Snf2. The structural characteristics of promoter chromatin during S phase expression are unknown. Furthermore, deletion of *SNF6*, which encodes a subunit of the SWI/SNF complex, reduced *PHO5* expression to 60% of wild-type expression (51).

The discrepancy between our results and those of others may be due to differences in genetic background, implying that the Pho4 activator recruits multiple factors that are each capable of catalyzing nucleosome disassembly. The inefficiency of competing activities would then have revealed SWI/SNF catalysis of nucleosome disassembly at *PHO5* in our strain background. This interpretation is consistent with a recent report that *PHO5* expression was marginally compromised in the absence of either Chd1 or Isw1, but abolished in the absence of both chromatin remodelers (25).

Delayed induction kinetics in mutant strains has frequently been construed as evidence of the importance of the missing factor for *PHO5* chromatin remodeling (24). However, such kinetic effects may also be due to defects in the PHO signaling pathway rather than nucleosome disassembly. This latter possibility was ruled out by the persistence of the disassembly defect in *pho80*Δ *snf2*Δ cells, but the possibility of an indirect effect of *SNF2* deletion on nucleosome disassembly cannot, by any means, be ruled out.

In vitro, SWI/SNF catalyzes the sliding of nucleosomes (8). The situation is less clear in the case of nucleosome disassembly. SWI/SNF has been seen to release histone H3 from chromatin templates that bore at least two nucleosomes (15), and RSC was found to disassemble mononucleosomes in the presence of the histone chaperone Nap1 (16). The ability of SWI/SNF and RSC to slide the histone octamer off the DNA end by up to 50 bp (52), however, raises the possibility that DNA ends may have played an important part in the mechanism of disassembly. *In vivo*, disassembly must occur in the absence of DNA ends. Optical tweezer experiments where DNA ends were blocked by attachment to polystyrene beads did not provide evidence for nucleosome disassembly by RSC or SWI/SNF (53). However, nucleosome disassembly may require specific histone modifications that are absent from *in vitro* reconstituted nucleosomes. A recent study of isolated *PHO5* chromatin gene circles showed that relaxation of repressed circles with topoisomerase after RSC treatment led to a linking change that matched complementary results for limiting digestion analysis of the circles, demonstrating that RSC removed nucleosomes from an end-less substrate (54). Similar results were obtained with promoter circles but not ORF circles, suggesting that disassembly was limited to promoter nucleosomes, which had to be marked specifically to allow for their removal. Indeed, treatment of circles with histone deacetylase diminished the removal of promoter nucleosomes by RSC (54). Our *in vivo* findings, together with the demonstration of promoter nucleosome disassembly by RSC in the absence of DNA ends, support the notion that SWI/SNF catalyzes the disassembly of promoter nucleosomes upon recruitment by activators *in vivo*.

How can this conclusion be reconciled with the conclusion that SWI/SNF catalyzes nucleosome sliding? An answer to this question is suggested by the notion that sliding of a nucleosome within the chromatin fiber unspools the DNA from its neighbor (55). Some evidence has been presented in support of this notion (15, 56, 57). Only nucleosomes marked by specific histone modifications may be conducive to this sliding-mediated disassembly (54). Loss of the crucial modifications may then limit the remodeler activity to sliding, which at *PHO5* is likely to result in repression of transcription because nucleosomes preferentially form over the transcription start sites rather than other sequences of the promoter (18). This might explain how SWI/SNF could function as a corepressor as well as coactivator of transcription (58), depending on the molecular context (see above).

The chromatin transitions at the *PHO8* and *PHO5* promoter are remarkably similar, pointing at the generality of our findings (18, 30). In both instances, activated promoter chromatin is generated by continual disassembly and reformation of nucleosomes. Of three promoter nucleosomes about two, on average, are removed upon Pho4 binding in each case, indicating that the ratio of the kinetic parameters for nucleosome disassembly and reassembly are about the same. The parameter values must be similar too, as we could correctly predict the magnitude of intrinsic *PHO8* expression noise on the basis of a stochastic model of chromatin remodeling and gene expression with kinetic parameters derived from *PHO5* expression noise and chromatin structure data (30). This only required adjustments in the kinetic parameters for transitions into and out of the transcriptionally active state to account for differences in steady-state expression between the two promoters.

Thus, we found that a lower frequency of promoter activation accounts mostly for the much reduced expression level of *PHO8* relative to *PHO5* (Fig. 6), suggesting that activated *PHO8* expression is due primarily to the acceleration of promoter nucleosome disassembly in contrast to *PHO5* where activator binding also accelerates the rate of promoter activation (30). As predicted by this assumption, we found a linear relationship between promoter nucleosome loss and *PHO8* expression level (Fig. 7*D*), whereas an exponential relationship was observed for *PHO5* (30).

How can the failure of Pho4 to stimulate the rate of promoter activation effectively at *PHO8* be explained? We note that the distance between the TATA box and the proximal Pho4 binding site (UASp2) of the *PHO8* promoter measures 400 bp, whereas Pho4 binding sites at the *PHO5* promoter are located 150 and 250 bp upstream of the TATA box. The distance between activator binding sites and the core promoter may be too large at *PHO8*, such that recruitment by activators would not increase the local concentration of recruited factors at the core promoter. In contrast, the efficiency of nucleosome disassembly at core promoter sequences may be relatively insensi-

tive to the distance between activator binding site and core promoter; disassembly of nucleosomes upon recruitment of SWI/SNF may reduce the nucleosome occupancy at a distant core promoter by subsequent sliding of nucleosomes toward the site of disassembly.

Shortening of the distance between UASp2 and the *PHO8* TATA box increased the level of *PHO8* expression (47), consistent with our expectation that the distance between UASp2 and the TATA box of *PHO8* is suboptimal for promoter activation. A suboptimal distance may be partially compensated for by a stronger affinity between the activator and the recruited factor, which would increase the dwell time of the factor at the promoter and thus its chance to interact with core promoter sequences. This might explain the deviation of the activator gain-of-function mutant D78A from our theoretical expectations (Fig. 7*D*).

Acknowledgments—We thank Drs. Craig Kaplan and Joachim Griesenbeck for critical comments on the manuscript and Dr. Fred Winston for plasmid pSR127. We also thank the UCSC MEGAMER facility and its manager Dr. Brandon Carter for assistance with flow cytometry.

REFERENCES

1. Griesenbeck, J., Boeger, H., Strattan, J. S., and Kornberg, R. D. (2003) *Mol. Cell. Biol.* **23,** 9275–9282
2. Han, M., and Grunstein, M. (1988) *Cell* **55,** 1137–1145
3. Kaplan, C. D., Laprade, L., and Winston, F. (2003) *Science* **301,** 1096–1099
4. Lorch, Y., LaPointe, J. W., and Kornberg, R. D. (1987) *Cell* **49,** 203–210
5. Mao, C., Brown, C. R., Griesenbeck, J., and Boeger, H. (2011) *PLoS One* **6,** e17521
6. Kornberg, R. D., and Lorch, Y. (1999) *Curr. Opin. Genet. Dev.* **9,** 148–151
7. Längst, G., Bonte, E. J., Corona, D. F., and Becker, P. B. (1999) *Cell* **97,** 843–852
8. Whitehouse, I., Flaus, A., Cairns, B. R., White, M. F., Workman, J. L., and Owen-Hughes, T. (1999) *Nature* **400,** 784–787
9. Fazzio, T. G., and Tsukiyama, T. (2003) *Mol. Cell* **12,** 1333–1340
10. Côté, J., Peterson, C. L., and Workman, J. L. (1998) *Proc. Natl. Acad. Sci. U.S.A.* **95,** 4947–4952
11. Lorch, Y., Cairns, B. R., Zhang, M., and Kornberg, R. D. (1998) *Cell* **94,** 29–34
12. Schnitzler, G., Sif, S., and Kingston, R. E. (1998) *Cell* **94,** 17–27
13. Lorch, Y., Zhang, M., and Kornberg, R. D. (1999) *Cell* **96,** 389–392
14. Phelan, M. L., Schnitzler, G. R., and Kingston, R. E. (2000) *Mol. Cell. Biol.* **20,** 6380–6389
15. Dechassa, M. L., Sabri, A., Pondugula, S., Kassabov, S. R., Chatterjee, N., Kladde, M. P., and Bartholomew, B. (2010) *Mol. Cell* **38,** 590–602
16. Lorch, Y., Maier-Davis, B., and Kornberg, R. D. (2006) *Proc. Natl. Acad. Sci. U.S.A.* **103,** 3090–3093
17. Almer, A., Rudolph, H., Hinnen, A., and Hörz, W. (1986) *EMBO J.* **5,** 2689–2696
18. Boeger, H., Griesenbeck, J., Strattan, J. S., and Kornberg, R. D. (2003) *Mol. Cell* **11,** 1587–1598
19. Reinke, H., and Hörz, W. (2003) *Mol. Cell* **11,** 1599–1607
20. Boeger, H., Griesenbeck, J., Strattan, J. S., and Kornberg, R. D. (2004) *Mol. Cell* **14,** 667–673
21. Gkikopoulos, T., Havas, K. M., Dewar, H., and Owen-Hughes, T. (2009) *Mol. Cell. Biol.* **29,** 4057–4066
22. Schwabish, M. A., and Struhl, K. (2007) *Mol. Cell. Biol.* **27,** 6987–6995
23. Takahata, S., Yu, Y., and Stillman, D. J. (2009) *Mol. Cell* **34,** 405–415
24. Barbaric, S., Luckenbach, T., Schmid, A., Blaschke, D., Hörz, W., and Korber, P. (2007) *J. Biol. Chem.* **282,** 27610–27621
25. Ehrensberger, A. H., and Kornberg, R. D. (2011) *Proc. Natl. Acad. Sci. U.S.A.* **108,** 10115–10120
26. Steger, D. J., Haswell, E. S., Miller, A. L., Wente, S. R., and O'Shea, E. K. (2003) *Science* **299,** 114–116
27. Gregory, P. D., Schmid, A., Zavari, M., Münsterkötter, M., and Hörz, W. (1999) *EMBO J.* **18,** 6407–6414
28. Adkins, M. W., Howar, S. R., and Tyler, J. K. (2004) *Mol. Cell* **14,** 657–666
29. Tyler, J. K., Adams, C. R., Chen, S. R., Kobayashi, R., Kamakaka, R. T., and Kadonaga, J. T. (1999) *Nature* **402,** 555–560
30. Mao, C., Brown, C. R., Falkovskaia, E., Dong, S., Hrabeta-Robinson, E., Wenger, L., and Boeger, H. (2010) *Mol. Syst. Biol.* **6,** 431
31. Ge, L., and Rudolph, P. (1997) *BioTechniques* **22,** 28–30
32. Almer, A., and Hörz, W. (1986) *EMBO J.* **5,** 2681–2687
33. Fascher, K. D., Schmitz, J., and Hörz, W. (1993) *J. Mol. Biol.* **231,** 658–667
34. Depew, D. E., and Wang, J. C. (1975) *Proc. Natl. Acad. Sci. U.S.A.* **72,** 4275–4279
35. Lenburg, M. E., and O'Shea, E. K. (1996) *Trends Biochem. Sci.* **21,** 383–387
36. Barbari, S., Fascher, K. D., and Hörz, W. (1992) *Nucleic Acids Res.* **20,** 1031–1038
37. Chaban, Y., Ezeokonkwo, C., Chung, W. H., Zhang, F., Kornberg, R. D., Maier-Davis, B., Lorch, Y., and Asturias, F. J. (2008) *Nat. Struct. Mol. Biol.* **15,** 1272–1277
38. Floer, M., Wang, X., Prabhu, V., Berrozpe, G., Narayan, S., Spagna, D., Alvarez, D., Kendall, J., Krasnitz, A., Stepansky, A., Hicks, J., Bryant, G. O., and Ptashne, M. (2010) *Cell* **141,** 407–418
39. Leschziner, A. E., Saha, A., Wittmeyer, J., Zhang, Y., Bustamante, C., Cairns, B. R., and Nogales, E. (2007) *Proc. Natl. Acad. Sci. U.S.A.* **104,** 4913–4918
40. Ansari, A., and Gartenberg, M. R. (1999) *Proc. Natl. Acad. Sci. U.S.A.* **96,** 343–348
41. Keller, W. (1975) *Proc. Natl. Acad. Sci. U.S.A.* **72,** 4876–4880
42. Prunell, A. (1998) *Biophys. J.* **74,** 2531–2544
43. Simpson, R. T., Thoma, F., and Brubaker, J. M. (1985) *Cell* **42,** 799–808
44. Svaren, J., Schmitz, J., and Hörz, W. (1994) *EMBO J.* **13,** 4856–4862
45. Dion, M. F., Kaplan, T., Kim, M., Buratowski, S., Friedman, N., and Rando, O. J. (2007) *Science* **315,** 1405–1408
46. Gaudreau, L., Schmid, A., Blaschke, D., Ptashne, M., and Hörz, W. (1997) *Cell* **89,** 55–62
47. Munsterkötter, M., Barbaric, S., and Hörz, W. (2000) *J. Biol. Chem.* **275,** 22678–22685
48. Swain, P. S., Elowitz, M. B., and Siggia, E. D. (2002) *Proc. Natl. Acad. Sci. U.S.A.* **99,** 12795–12800
49. Elowitz, M. B., Levine, A. J., Siggia, E. D., and Swain, P. S. (2002) *Science* **297,** 1183–1186
50. Neef, D. W., and Kladde, M. P. (2003) *Mol. Cell. Biol.* **23,** 3788–3797
51. Raser, J. M., and O'Shea, E. K. (2004) *Science* **304,** 1811–1814
52. Flaus, A., and Owen-Hughes, T. (2003) *Mol. Cell. Biol.* **23,** 7767–7779
53. Zhang, Y., Smith, C. L., Saha, A., Grill, S. W., Mihardja, S., Smith, S. B., Cairns, B. R., Peterson, C. L., and Bustamante, C. (2006) *Mol. Cell* **24,** 559–568
54. Lorch, Y., Griesenbeck, J., Boeger, H., Maier-Davis, B., and Kornberg, R. D. (2011) *Nat. Struct. Mol. Biol.* **18,** 881–885
55. Cairns, B. R. (2007) *Nat. Struct. Mol. Biol.* **14,** 989–996
56. Boeger, H., Griesenbeck, J., and Kornberg, R. D. (2008) *Cell* **133,** 716–726
57. Engeholm, M., de Jager, M., Flaus, A., Brenk, R., van Noort, J., and Owen-Hughes, T. (2009) *Nat. Struct. Mol. Biol.* **16,** 151–158
58. Holstege, F. C., Jennings, E. G., Wyrick, J. J., Lee, T. I., Hengartner, C. J., Green, M. R., Golub, T. R., Lander, E. S., and Young, R. A. (1998) *Cell* **95,** 717–728
59. Svaren, J., and Hörz, W. (1997) *Trends Biochem. Sci* **22,** 93–97